Autophagy is required in macrophages and dendritic cells to prevent early recruitment of neutrophils during *Mycobacterium tuberculosis* infection

Rachel L. Kinsella*, Jacqueline M. Kimmey[#], Asya Smirnov, Reilly Woodson, Margaret R. Gaggioli, Sthefany M. Chavez, Darren Kreamalmeyer, Christina L. Stallings*

Department of Molecular Microbiology, Center for Women's Infectious Disease Research, Washington University School of Medicine, St. Louis, MO 63110, USA

[#]Current address: Department of Microbiology and Environmental Toxicology, UC Santa Cruz, Santa Cruz, CA, USA

*Correspondence:

Rachel L. Kinsella: rlkinsella@wustl.edu, 314-286-0277

Christina L. Stallings: stallings@wustl.edu, 314-286-0276

Keywords: autophagy, *Mycobacterium tuberculosis*, macrophage, dendritic cells, neutrophils, inflammation, T_H17

Running title: Autophagy prevents neutrophil accumulation during infection

[¶]This work was supported by NIH grants R01 AI132697 and U19 AI142784, a Burroughs Wellcome Fund Investigators in the Pathogenesis of Infectious Disease Award, and the Philip and Sima Needleman Center for Autophagy Therapeutics and Research to C.L.S., a Potts Memorial Foundation postdoctoral fellowship to R.L.K., and a National Science Foundation Graduate Research Fellowship DGE-1143954 and the NIGMS Cell and Molecular Biology Training Grant GM007067 to J.M.K.

ABSTRACT

The immune response to *Mycobacterium tuberculosis* infection determines tuberculosis disease outcomes, yet we have an incomplete understanding of what immune factors contribute to a protective immune response. Neutrophilic inflammation has been associated with poor disease prognosis in humans and in animal models during *M. tuberculosis* infection and, therefore, must be tightly regulated. ATG5 is an essential autophagy protein that is required in innate immune cells to control neutrophil-dominated inflammation and promote survival during *M. tuberculosis* infection, however, the mechanistic basis for how ATG5 regulates neutrophil recruitment is unknown. To interrogate what innate immune cells require ATG5 to control neutrophil recruitment during *M. tuberculosis* infection, we used different mouse strains that conditionally delete *Atg5* in specific cell types. We found that ATG5 is required in $CD11c^+$ cells (lung macrophages and dendritic cells) to control the production of proinflammatory cytokines and chemokines during *M. tuberculosis* infection, which would otherwise promote neutrophil recruitment. This role for ATG5 is autophagy-dependent, but independent of mitophagy, LC3-associated phagocytosis, and inflammasome activation, which are the most well-characterized ways that autophagy proteins regulate inflammation. In addition to the increase in proinflammatory cytokine production during *M. tuberculosis* infection, loss of ATG5 in innate immune cells also results in an early induction of T_H17 responses. These findings reveal new roles for autophagy proteins in lung resident macrophages and dendritic cells that are required to suppress inflammatory responses that are associated with poor control of *M. tuberculosis* infection.

INTRODUCTION

According to the World Health Organization, 10 million people fell ill with *Mycobacterium tuberculosis* infection and 1.5 million people died of tuberculosis (TB) in 2020, marking the first increase in TB-associated deaths in over a decade(1). Whether a person controls the initial *M. tuberculosis* infection or develops active TB disease is directly impacted by the type of immune response elicited in the infected individual(2). Therefore, better understanding of what constitutes a protective versus non-protective immune response to *M. tuberculosis* infection is critical for developing better therapies and prevention measures to fight this deadly disease. Genetic mouse models have provided invaluable insight into the immunological processes that are required for control of *M. tuberculosis* infection. Infection of mice through the aerosol route leads to phagocytosis of *M. tuberculosis* by alveolar macrophages, initiating an inflammatory response and recruitment of innate immune cells to the lung(2). *M. tuberculosis* replicates within these innate immune cells until antigen specific T cells traffic to the lung where they activate the innate immune cells to restrain *M. tuberculosis* replication and suppress inflammation. *M. tuberculosis* establishes a chronic infection in wild-type (WT) mice, which can survive for over a year with this infection.

Atg5$^{fl/fl}$*-LysM-Cre* mice, which delete the *Atg5* gene specifically in macrophages, inflammatory monocytes, some dendritic cells (DCs), and neutrophils, are severely susceptible to *M. tuberculosis* infection(3–5), highlighting ATG5 as a critical component of a protective immune response to *M. tuberculosis*. *M. tuberculosis* infected *Atg5*$^{fl/fl}$*-LysM-Cre* mice fail to control bacterial replication and succumb to infection by 40 days post-infection (dpi)(3–5). The uncontrolled *M. tuberculosis* replication is associated with an early (by 14 dpi) and sustained influx of neutrophils to the lungs of the infected *Atg5*$^{fl/fl}$*-LysM-Cre* mice. Depletion of neutrophils during *M. tuberculosis* infection in *Atg5*$^{fl/fl}$*-LysM-Cre* mice extends their survival(3), demonstrating that the neutrophil-dominated inflammation contributed to their susceptibility. In general, higher abundances of neutrophils during *M. tuberculosis* infection have been associated with worse disease outcomes in mice (6–13) and humans (12, 14–17). Therefore, understanding the regulatory mechanisms that govern neutrophil recruitment

and accumulation during *M. tuberculosis* infection could be key for manipulating inflammatory responses to better control TB.

ATG5 is required for the intracellular pathway of autophagy, a process by which cytoplasmic contents are targeted to the lysosome for degradation(18, 19). Initiation of autophagy involves phagophore formation from the endoplasmic reticulum, which is mediated by the ULK1 complex (ULK1/ULK2, ATG13, FIP200, ATG101) and the PI3 kinase complex (ATG14L, BECLIN1, VPS15, and VPS34)(20, 21). Elongation of the autophagosomal double membrane depends on two ubiquitin-like conjugation systems. In the first system, ATG12 is activated by ATG7, transferred to ATG10, and covalently attached to ATG5. The second ubiquitin-like component is LC3 (microtubule-associated protein 1 light chain 3), which is conjugated to phosphatidylethanolamine, generating the membrane bound form called LC3-II through the actions of ATG7 and ATG3. ATG5-ATG12 facilitates LC3 lipidation through its interactions with ATG3, while ATG16L1 specifies the localization of LC3 conjugation to the autophagosome membrane(18, 19, 21, 22). The autophagosome membrane is then completed and targeted for fusion with the lysosome, where the autophagosome cargo are degraded. However, ATG5 also functions outside of autophagy, including during *M. tuberculosis* infection(3), although these activities remain poorly understood. The mechanistic basis for how loss of ATG5 results in early and exagerated recruitment of neutrophils during *M. tuberculosis* infection and whether this activity for ATG5 involves autophagy remains unknown.

In this manuscript, we dissect the role for ATG5 in regulating neutrophil recruitment and accumulation during *M. tuberculosis* infection. We find that ATG5 functions with other autophagy proteins in $CD11c^+$ lung macrophages and DCs to limit proinflammatory responses that otherwise promote neutrophil influx to the lung early in *M. tuberculosis* infection. In addition, ATG5 is required in lung macrophages and DCs to limit IL-17A production from $CD4^+$ T cells. Therefore, our studies reveal new roles for ATG5 and other autophagy proteins in regulating inflammatory responses during infection, which with further dissection could provide insight into pathways that may be targeted to effectively promote protective immune responses during TB.

MATERIALS AND METHODS

Mice

All flox mice (*Atg5*$^{fl/fl}$, *Atg16l1*$^{fl/fl}$, *Becn1*$^{fl/fl}$) used in this study have been described previously (3, 23, 24) and colonies are maintained in an enhanced barrier facility. LysM-Cre (Jax #004781), Cd11c-Cre (Jax #007567), Mrp8-Cre (Jax #021614) from the Jackson Laboratory were crossed to specific flox mice. *Il17a-IRES-GFP-KI* (Jax # 018472) reporter mice were bred to *Atg5*$^{fl/fl}$*-LysM-Cre* and *Atg5*$^{fl/fl}$ mice to generate the *Il17a-GFP/Atg5*$^{fl/fl}$*-LysM-Cre* and *Il17a-GFP/Atg5*$^{fl/fl}$ lines. *Rubicon*$^{-/-}$ (Jax # 032581) mice were provided by Drs. Douglas Green and Jennifer Martinez (25). Caspase 1/11$^{-/-}$ (Jax #016621) were bred to *Atg5*$^{fl/fl}$*-LysM-Cre* and *Becn1*$^{fl/fl}$*-LysM-Cre* mice. *Parkin*$^{-/-}$ (Jax # 006582)(26), *Pink1*$^{-/-}$ (Jax # 017946)(27) and WT control mice were provided by Dr. Jonathan Brestoff at Washington University School of Medicine. Male and female littermates (aged 6-12 weeks) were used and were subject to randomization. A minimum of 3 mice were used per experiment and each experiment was performed twice. Statistical consideration was not used to determine mouse sample sizes. The mice were housed and bred at Washington University in St. Louis in specific pathogen-free conditions in accordance with federal and university guidelines, and protocols were approved by the Animal Studies Committee of Washington University.

Infection of mice with *M. tuberculosis* and measurement of bacterial burden in the lungs

M. tuberculosis Erdman expressing GFP (10, 28) was used in all experiments except experiments with the *Il-17a-GFP*/*Atg5*$^{fl/fl}$*-LysM-Cre* reporter mice when WT Erdman was used. *M. tuberculosis* was cultured at 37°C in 7H9 (broth) or 7H11 (agar) (Difco) medium supplemented with 10% oleic acid/albumin/dextrose/catalase (OADC), 0.5% glycerol, and 0.05% Tween 80 (broth). Cultures of GFP expressing *M. tuberculosis* were grown in the presence of kanamycin (20μg/mL) to ensure plasmid retention. *M. tuberculosis* cultures in logarithmic growth phase (OD600 = 0.5–0.8) were washed with PBS + 0.05% Tween-80, sonicated to disperse clumps, and diluted in sterile water before delivering 100 CFUs of aerosolized *M. tuberculosis* per lung using an Inhalation Exposure System (Glas-Col). Within 2 hours of each infection, lungs were harvested from at least two control mice,

homogenized, and plated on 7H11 agar to determine the input CFU dose. At 14 dpi, *M. tuberculosis* titers were determined by homogenizing the superior, middle, and inferior lobes of the right lung and plating serial dilutions on 7H11 agar. Colonies were counted after 3 weeks of incubation at 37°C in 5% CO2.

Flow cytometry from infected lungs

Lungs were perfused with sterile PBS and digested for 1 hour with 625µg/mL collagenase D (Roche 11088875103) and 75U/mL DNase I (Sigma D4527). Cells were quenched with PBS + 2% heat-inactivated (HI)-FBS, + 2mM EDTA and passed through a 70µM filter. Cells were suspended in PBS + 2% HI-FBS + 2mM EDTA in the presence of Fc receptor blocking antibody (BioLegend, 101302) and stained with antibodies at a 1:200 dilution against the following mouse markers: CD11b_BV605 or PerCP-Cy5.5 (clone M1/70), CD45_AF700 (BioLegend, 103259), Ly6G_PE-Cy7 or AF647 (clone 1A8), MHCII_Spark blue 550 (BioLegend, 107662), CD62L_Pe/Cy5 (BioLegend, 104410), CD44_BV510 (BioLegend, 103044), CD11c_PerCP (BioLegend, 117325), Ly6C_BV605 (BioLegend, 128036), CD4_BV570 (clone RM4-5), TCRb_BV421 (clone H57-597), CD19_Pacific blue (Zombie-NIR (Biolegend, 423105), CD64_PerCP-eFluor 710 (eBiosciences, 46061482) and Mertk_PE/Cy7 (eBiosciences, 25575182). Cells were stained for 20 minutes at 4ºC and then fixed in 4% paraformaldehyde (Electron Microscope Sciences) for 20 minutes at room temperature. Flow cytometry was performed on an LSR-Fortessa (BD Bioscience) or an Aurora (Cytek Biosciences, with 4 laser 16V-14B-10YG-8R configuration) and analyzed using FlowJo software (Tree Star). Absolute cell counts were determined using Precision count beads (BioLegend) or volumetric-based counting on the Aurora. Gating strategies to identify neutrophils, $CD4^+$ T cells and IL-17-GFP^+ $CD4^+$ T cells are in Supplementary Figure 1.

Culturing and infection of bone marrow derived macrophages (BMDMs)

BMDMs were generated by flushing femurs and tibias of mice and culturing the cells in DMEM, 20% HI-FBS, 10% supernatant from 3T3 cells overexpressing M-CSF + 1% MEM non-essential amino acids (Cellgro 25-025-CI), 2mM L-glutamine, 100U/mL penicillin and 100µg/mL streptomycin (Sigma P4333) at 37ºC in 5% CO_2 in

non-TC treated plates. After 6 days non-adherent cells were removed and $1x10^6$ adherent macrophages were seeded per well in 6 well non-TC treated plates in DMEM, 10% HI-FBS, 1% MEM non-essential amino acids and 2 mM L-glutamine. BMDMs were rested overnight at 37°C in 5% CO_2. *M. tuberculosis* was grown to an OD of 0.6-0.8, washed with PBS twice, sonicated to disperse clumps, centrifuged at 55xg for 10 minutes to remove clumps and resuspended in antibiotic-free BMDM media. Macrophages were infected at an MOI of 10 by centrifuging the cells at 200xg for 10 minutes. BMDMs were washed with PBS twice to remove unbound *M. tuberculosis* and fresh BMDM media was added to each well. Cells were incubated at 37°C and 5% CO_2 for 24 hours. To determine CFU counts, the cells were lysed with 0.05% triton X-100, serially diluted, and plated onto 7H11 agar and incubated for 21 days when bacterial colonies were counted. At 24 hours post-infection (hpi) supernatants were stored at -80°C for cytokine analysis.

Cytokine analysis

BMDM supernatants were filtered through a 0.22 µm filter twice to remove *M. tuberculosis* and analyzed using the BioPlex-Pro Mouse Cytokine 23-Plex Immunoassay (Bio-Rad) as per the manufacturer's instructions. ELISAs were performed according to the manufacturer's instructions (R&D systems): KC/CXCL1 (DY453), IL-6 (DY406) and G-CSF (DY414).

IL-17A blocking and T cell depletion

To neutralize IL-17A, 100µg of InVivo monoclonal anti-IL-17A (Bio X Cell, BE0173) neutralizing antibody was administered to *Atg5*$^{fl/fl}$ and *Atg5*$^{fl/fl}$*-LysM-Cre* mice by intraperitoneal (i.p.) injection every other day starting at 1 day prior to infection, with the final dose delivered at 13 dpi, similar to published protocols (29). Control mice received 100µg of IgG from mouse serum (Sigma, I5381) by i.p. injection every other day starting 1 day prior to infection and finishing on 13 dpi. To deplete $CD4^+$ T cells from mice, 250µg of anti-mouse CD4 (Leinco Technologies, C1333) was administered by i.p. injection at 2 days prior to infection, 5 dpi and 12 dpi. Control mice received 250µg of IgG from rat serum (Sigma, 18015) i.p. on 2 days prior to infection, 5 dpi and 12 dpi.

Data and statistics

All experiments were performed at least twice. When shown, multiple samples represent biological (not technical) replicates of mice randomly sorted into each experimental group. No blinding was performed during animal experiments. Animals were only excluded when pathology unrelated to *M. tuberculosis* infection was present (i.e. bad teeth leading to weight loss). Determination of statistical differences was performed with Prism (GraphPad Software, Inc.) using log-rank Mantel-Cox test (survival), unpaired two-tailed t-test (to compare two groups with similar variances), or one-way ANOVA with Šídák Multiple Comparison test (to compare more than two groups). When used, center values and error bars represent the mean +/- S.E.M. In all figures, all significant differences are indicated by asterisks: * $P<0.05$, ** $P<0.01$, *** $P<0.001$, **** $P<0.0001$. Non-significant comparisons of particular interest are noted as n.s. (not significant).

RESULTS

ATG5 is required in CD11c$^+$ lung macrophages and DCs to control neutrophil recruitment and accumulation early during *M. tuberculosis* infection *in vivo*.

M. tuberculosis infection of *Atg5$^{fl/fl}$-LysM-Cre* mice results in the recruitment of a higher number of neutrophils in the lungs at 14 dpi as compared to *Atg5$^{fl/fl}$* controls, despite equivalent bacterial burdens at this time point (3). This indicates that the neutrophils are accumulating due to a defect in inflammatory responses to infection and not due to higher burden. There are also no differences in the abundance of other cell types in *Atg5$^{fl/fl}$-LysM-Cre* and *Atg5$^{fl/fl}$* mice at 14 dpi (3). To determine which LysM$^+$ cells required ATG5 to control the early influx of neutrophils into the lungs during *M. tuberculosis* infection, we compared bacterial burdens and neutrophil inflammation in *Atg5$^{fl/fl}$-LysM-Cre*, *Atg5$^{fl/fl}$-Mrp8-Cre* (deletion in neutrophils), *Atg5$^{fl/fl}$-Cd11c-Cre* (deletion in lung resident macrophages and DCs), and *Atg5$^{fl/fl}$* controls at 14 dpi. At 14 dpi, the *Atg5$^{fl/fl}$-LysM-Cre* and *Atg5$^{fl/fl}$-Cd11c-Cre* mice, but not *Atg5$^{fl/fl}$-Mrp8-Cre* mice, had higher levels of neutrophil inflammation in the lungs as compared to *Atg5$^{fl/fl}$* controls **(Fig. 1A and B)**. The degree of increased neutrophil frequency was similar in *Atg5$^{fl/fl}$-LysM-Cre* and *Atg5$^{fl/fl}$-Cd11c-Cre* mice, demonstrating that loss of *Atg5* in CD11c$^+$ cells, but not neutrophils, leads to the early influx of neutrophils into the lungs during *M. tuberculosis* infection. At 14 dpi, none of the mouse strains harbored increased *M. tuberculosis* burden in their lungs **(Fig. 1C)**, indicating that the increase in neutrophil abundance in *Atg5$^{fl/fl}$-Cd11c-Cre* mice is not due to elevated bacterial burden and reflects a dysregulated inflammatory response to infection.

The higher levels of neutrophils in the lungs of *Atg5$^{fl/fl}$-LysM-Cre* and *Atg5$^{fl/fl}$-Cd11c-Cre* mice were sustained through 21dpi **(Fig. 1D)**. However, only *Atg5$^{fl/fl}$-LysM-Cre* mice, and not *Atg5$^{fl/fl}$-Cd11c-Cre* mice, had higher bacterial burdens in the lungs at 21 dpi **(Fig. 1E)**, similar to previously reported (3). Loss of *Atg5* in neutrophils results in increased susceptibility to *M. tuberculosis* infection in some, but not all, *Atg5$^{fl/fl}$-Mrp8-Cre* mice (3). The susceptible *Atg5$^{fl/fl}$-Mrp8-Cre* mice accumulate higher neutrophil numbers and bacterial burdens in their lungs at 21 dpi **(Fig. 1D and E)**(3). Therefore, loss of *Atg5* in neutrophils is likely contributing to the higher burdens in the lungs of *Atg5$^{fl/fl}$-LysM-Cre* mice at 21 dpi. These data indicate that ATG5 has a role in CD11c$^+$

lung macrophages and DCs to regulate early recruitment of neutrophils, but not the control of *M. tuberculosis* replication at 14 and 21 dpi.

To determine how the loss of Atg5 in $CD11c^+$ cells and the resulting early influx of neutrophils into the lungs affected host susceptibility, we monitored survival in *M. tuberculosis* infected *Atg5$^{fl/fl}$-Cd11c-Cre* mice as compared to *Atg5$^{fl/fl}$* controls. *Atg5$^{fl/fl}$-Cd11c-Cre* mice succumbed to *M. tuberculosis* infection between 100 and 150 dpi, which was significantly earlier than *Atg5$^{fl/fl}$* controls (median survival time of 259 dpi) **(Fig. 1F)**, but not as early as *Atg5$^{fl/fl}$-LysM-Cre* mice (succumb 30-40 dpi (3)). These data demonstrate that ATG5 is required in $CD11c^+$ lung macrophages and DCs to control early neutrophil recruitment and promote survival following *M. tuberculosis* infection.

The role for ATG5 in macrophages and DCs in regulating neutrophil recruitment is dependent on other autophagy proteins.

We previously showed that at least one role for ATG5 in innate immune cells to control *M. tuberculosis* infection is autophagy-independent (3). To determine whether the regulation of neutrophil recruitment by ATG5 in $CD11c^+$ lung macrophages and DCs was dependent on other autophagy proteins or represented the autophagy-independent role for ATG5 during *M. tuberculosis* infection, we monitored neutrophil abundance in the lungs of mice lacking expression of another essential autophagy protein, BECLIN 1, in $CD11c^+$ cells (*Becn1$^{fl/fl}$-Cd11c-Cre*) at 14 dpi by flow cytometry. Similar to *Atg5$^{fl/fl}$-Cd11c-Cre* mice, *Becn1$^{fl/fl}$-Cd11c-Cre* mice also exhibited elevated neutrophil frequency in the lung at 14 dpi relative to *Becn1$^{fl/fl}$* control mice **(Fig. 2A)**, despite no difference in bacterial burden **(Fig. 2B)**. In addition, analysis of *M. tuberculosis* infected *Atg16l1$^{fl/fl}$-LysM-Cre* and *Becn1$^{fl/fl}$-LysM-Cre* mice also revealed higher levels of neutrophils in the lungs at 14 dpi relative to controls, without higher bacterial burdens **(Fig. 2C and D)**.

In addition to their role in canonical autophagy, the proteins ATG5, BECLIN 1, and ATG16L1 are also required for the process of LC3 associated phagocytosis (LAP), where LC3 is recruited to the phagosome, resulting in $LC3^+$ single membrane vesicles that traffic to the lysosome for degradation. LAP can dampen

inflammatory responses through efferocytosis, pathogen removal, stimulating inhibitory immune-receptor signaling, and reducing auto-antigen levels (30–32). In contrast to canonical autophagy, LAP uses RUBICON and UVRAG instead of ATG14 in the PI3K complex and does not depend on ULK1 (30, 33, 34). To distinguish between whether ATG5, BECLIN 1, and ATG16L1 were functioning through autophagy or LAP to regulate neutrophil recruitment during *M. tuberculosis* infection, we infected mice lacking RUBICON expression, a protein specifically required for LAP. *Rubicon*$^{-/-}$ mice had no difference in neutrophil accumulation or bacterial burdens as compared to WT controls following *M. tuberculosis* infection **(Fig. 2C and D)**, indicating that LAP is not required to control neutrophil inflammation during *M. tuberculosis* infection. Importantly, BECLIN 1 and ATG5 function at different steps of autophagy. Therefore, the requirement of both BECLIN 1 and ATG5 suggests that both the initiation and elongation steps of autophagy are required in CD11c^{+} cells to control neutrophil recruitment early during *M. tuberculosis* infection.

Autophagy regulates proinflammatory responses in macrophages during *M. tuberculosis* infection.

Up to 14 dpi, the primary CD11c^{+} cell types that are infected by *M. tuberculosis* are the lung resident macrophages (35, 36). The absence of differences in *M. tuberculosis* lung burden in *Atg5*$^{fl/fl}$*-Cd11c-Cre* and *Atg5*$^{fl/fl}$ mice at 14 dpi indicates that autophagy is not required to control *M. tuberculosis* replication in macrophages. Therefore, the role of autophagy in CD11c^{+} cells could be to regulate signals that recruit neutrophils. We have previously shown that lungs of *Atg5*$^{fl/fl}$*-LysM-Cre* mice at 14 dpi contain higher levels of G-CSF and IL-17A than control mice (3), cytokines that promote neutrophil development and recruitment. Therefore, we hypothesized that autophagy could be suppressing the production of these cytokines from *M. tuberculosis* infected macrophages. We tested this hypothesis by culturing bone marrow derived macrophages (BMDMs) from *Atg5*$^{fl/fl}$, *Atg5*$^{fl/fl}$*-LysM-Cre*, *Atg16l1*$^{fl/fl}$, *Atg16l1*$^{fl/fl}$*-LysM-Cre*, *Becn1*$^{fl/fl}$, and *Becn1*$^{fl/fl}$*-LysM-Cre* mice and infecting with *M. tuberculosis in vitro* before monitoring cytokine and chemokine production using a cytokine bead array (Bio-Rad) on the supernatants from infected cultures. Of the 23 cytokines tested, we detected significantly higher levels of IL-1β, G-CSF, KC, TNF-α and RANTES from the *Atg5*$^{fl/fl}$*-LysM-Cre* macrophage cultures compared to controls at 24

hpi **(Fig. 3A-F),** despite no difference in bacterial burdens at this time point **(Fig. 3G)**. The levels of these cytokines were only different following *M. tuberculosis* infection and not in mock infected cultures, indicating that the increased pro-inflammatory responses were infection-induced. The higher levels of G-CSF and KC, both pro-inflammatory signals associated with neutrophil inflammation (37–39), produced from *Atg5*-deficient macrophages in response to *M. tuberculosis* infection was dose dependent and confirmed by ELISA **(Fig. 3H-I)**. Similar to *Atg5$^{fl/fl}$-LysM-Cre* BMDMs, *Atg16l1$^{fl/fl}$-LysM-Cre* BMDMs also produced higher levels of G-CSF, TNF-α and IL-1β following *M. tuberculosis* infection *in vitro* **(Fig. 3A-F)**. *Becn1$^{fl/fl}$-LysM-Cre* BMDMs also produced more G-CSF and IL-1β following *M. tuberculosis* infection *in vitro* compared to control cells (**Fig. 3A-F**) despite no difference in *M. tuberculosis* burden at this time point (**Fig. 3G**). In addition, *Becn1$^{fl/fl}$-LysM-Cre* BMDMs produced higher levels of IL-6, MIP-1α, MIP-1β, and MCP-1 following *M. tuberculosis* infection (**Fig. 3C, Supplemental Fig. 2**). IL-6 in particular is associated with neutrophil recruitment (40–43) and also trended higher in *M. tuberculosis*-infected *Atg5$^{fl/fl}$-LysM-Cre* BMDMs, so we further analyzed the levels of IL-6 produced by *M. tuberculosis*-infected *Atg5$^{fl/fl}$-LysM-Cre* BMDMs using an ELISA. These analyses revealed a dose-dependent increase of IL-6 secretion in *M. tuberculosis*-infected *Atg5$^{fl/fl}$-LysM-Cre* BMDMs. Together these data show that loss of expression of the autophagy proteins ATG5, ATG16L1, and BECLIN 1 results in higher levels of cytokines and chemokines that are associated with neutrophil recruitment and accumulation following *M. tuberculosis* infection relative to controls, indicating that canonical autophagy is required in macrophages to control proinflammatory responses during *M. tuberculosis* infection.

Autophagy suppresses neutrophil recruitment early during *M. tuberculosis* infection independent of mitophagy and inflammasome activation.

Autophagy has been shown to suppress proinflammatory responses by negatively regulating inflammasome activation indirectly through regulation of NFκB signaling and directly by degrading pro-IL-1β and inflammasome components (44), which can otherwise promote pro-inflammatory responses, IL-1β secretion, and neutrophil recruitment (44–48). Indeed, *Atg5$^{fl/fl}$-LysM-Cre*, *Atg16l1$^{fl/fl}$-LysM-Cre* and *Becn1$^{fl/fl}$-LysM-Cre*

BMDMs produce significantly more IL-1β in response to *M. tuberculosis* infection *in vitro* at 24 hpi compared to control BMDMs (**Fig. 3A**), supporting that loss of autophagy has resulted in increased inflammasome activation. The primary inflammasome activated during *M. tuberculosis* infection of macrophages is the NLRP3 inflammasome, which consists of the NOD-, LRR- and pyrin-domain containing protein 3 (NLRP3) sensor, ASC adaptor, and caspase 1 (49–52). TLR engagement and NFκB activation during *M. tuberculosis* infection constitute the priming step of inflammasome activation, resulting in increased expression of pro-IL-1β and NLRP3 (53, 54). Phagocytosis of *M. tuberculosis* and subsequent Esx-1-dependent plasma membrane damage leading to potassium efflux is the second signal promoting NLRP3 inflammasome formation, which mediates CASPASE 1 activation followed by IL-1β processing and secretion (26, 29).

To determine whether the increased neutrophil inflammation following *M. tuberculosis* infection in autophagy-deficient mice results from increased inflammasome activation, we crossed *Caspase1/11*$^{-/-}$ mice to *Atg5*$^{fl/fl}$*-LysM-Cre* and *Becn1*$^{fl/fl}$*-LysM-Cre* mice and monitored neutrophil abundance in the lungs at 14 dpi. *Caspase1/11*$^{-/-}$*/Atg5*$^{fl/fl}$*-LysM-Cre and Caspase1/11*$^{-/-}$*/Becn1*$^{fl/fl}$*-LysM-Cre* mice had similar neutrophil abundances and bacterial burdens in the lungs at 14 dpi as *Atg5*$^{fl/fl}$*-LysM-Cre mice* and *Becn1*$^{fl/fl}$*-LysM-Cre* mice, respectively **(Fig. 4A-B)**, indicating that increased neutrophil recruitment in the absence of autophagy occurs independent of CASPASE1/11. *Caspase1/11* deletion also did not extend the survival of *Atg5*$^{fl/fl}$*-LysM-Cre* mice, indicating that increased inflammasome activation does not contribute to the early susceptibility of these mice **(Fig. 4C)**.

Autophagy has also been shown to suppress inflammatory responses via the process of mitophagy, where autophagy targets old and damaged mitochondria to the lysosome for degradation (27, 55). The build-up of damaged or dysfunctional mitochondria in the absence of autophagy results in loss of mitochondrial membrane potential and the release of reactive oxygen species (ROS), mitochondrial DNA, and ATP to the cytosol where it can lead to oxidative damage, inflammasome activation, and pro-inflammatory cytokine production (55–59). Mitophagy requires the canonical autophagy proteins, including ATG5, ATG16L1, and BECLIN 1, as well as PARKIN and PTEN-induced kinase 1 (PINK1)(60). PINK1 accumulates on damaged mitochondria and activates the mitochondrial E3 ubiquitin ligase, PARKIN, to ubiquitinylate damaged mitochondria (56, 59). Optineurin and

NDP52 are the main mitophagy receptors that interact with the ubiquitinylated mitochondria and LC3 leading to autophagosome engulfment of the mitochondria (56, 61). To investigate whether loss of mitophagy could contribute to higher neutrophil accumulation in the lungs following *M. tuberculosis* infection, we measured neutrophil frequency in the lung at 14 dpi by flow cytometry in *Parkin*$^{-/-}$ and *Pink1*$^{-/-}$ mice relative to WT controls. There was no difference in neutrophil abundance or bacterial burdens in *M. tuberculosis*-infected *Parkin*$^{-/-}$ or *Pink1*$^{-/-}$ mice relative to WT mice at 14 dpi **(Fig. 4D-E)**, indicating that mitophagy is not required to control neutrophil recruitment early during *M. tuberculosis* infection. To determine if mitophagy is required in macrophages to control proinflammatory cytokine and chemokine production during *M. tuberculosis* infection we generated BMDMs from *Parkin*$^{-/-}$, *Pink1*$^{-/-}$, and WT mice and infected the macrophages with *M. tuberculosis* for 24 hours. We measured cytokine and chemokine levels from mock and *M. tuberculosis* infected cultures using the cytokine bead array (Bio-Rad). Unlike in autophagy-deficient BMDMs, there were no differences in IL-6, IL-1β, G-CSF, KC, TNF-α or RANTES production by *M. tuberculosis* infected *Parkin*$^{-/-}$ and *Pink1*$^{-/-}$ macrophages at 24 hpi compared with WT macrophages (**Supplemental Fig. 3**), nor any differences in bacterial burden (**Supplemental Fig. 3**). Therefore, loss of mitophagy in macrophages does not result in higher levels of inflammation during *M. tuberculosis* infection.

ATG5 is required to suppress early T$_H$17 responses in the lungs during *M. tuberculosis* infection.

The higher levels of IL-17A observed in the lungs of *Atg5*$^{fl/fl}$*-LysM-Cre* mice at 14 dpi with *M. tuberculosis* relative to controls was not reproduced by BMDMs infected with *M. tuberculosis* for 24 hours (**Supplementary Fig. 2)**. Although there are many possible explanations for this, one possibility is that the macrophages were not the source of IL-17A *in vivo*. We investigated what cell type was expressing higher levels of IL-17A in the *Atg5*$^{fl/fl}$*-LysM-Cre* mice during *M. tuberculosis* infection by crossing the *Atg5*$^{fl/fl}$ and *Atg5*$^{fl/fl}$*-LysM-Cre* mice with an IL-17A reporter mouse that expresses GFP under the IL-17A promoter (*Il17a-GFP*, Jax #018472). We infected *Il17a-GFP/Atg5*$^{fl/fl}$ and *Il17a-GFP/Atg5*$^{fl/fl}$*-LysM-Cre* mice with *M. tuberculosis* and monitored GFP expression as a proxy of IL-17A expression in immune cells at 14 dpi. The only cell type we reproducibly detected >0.5%

of the cells expressing GFP were CD4$^+$ T cells. Similar to previous studies with *Atg5$^{fl/fl}$* and *Atg5$^{fl/fl}$-LysM-Cre* mice, there was no difference in total CD4$^+$ T cell numbers in the lungs of *Il17a-GFP/Atg5$^{fl/fl}$* and *Il17a-GFP/Atg5$^{fl/fl}$-LysM-Cre* mice at 14 dpi **(Fig. 5A)** (3). However, a greater frequency and number of the CD4$^+$ T cells in the lungs of *Il17a-GFP/Atg5$^{fl/fl}$-LysM-Cre* mice at 14 dpi were IL-17-GFP$^+$ compared to *Il17a-GFP/Atg5$^{fl/fl}$* mice **(Fig. 5B-C)**. These data indicate that CD4$^+$ T cells contribute to the higher levels of IL-17A in the lungs of *M. tuberculosis* infected *Atg5$^{fl/fl}$-LysM-Cre* mice and ATG5 is required in innate immune cells to negatively regulate T_H17 responses during *M. tuberculosis* infection.

IL-17A drives neutrophil influx by promoting the production of neutrophil chemokines MIP-1α and KC and through activation of endothelial cells (62–64). Therefore, the increased T_H17 responses could be responsible for the early influx and accumulation of neutrophils in the lungs of *M. tuberculosis*-infected *Atg5$^{fl/fl}$-LysM-Cre* mice. To determine if the increased expression of IL-17A by T cells was responsible for the enhanced influx of neutrophils at 14 dpi in *Atg5$^{fl/fl}$-LysM-Cre* mice, we depleted CD4$^+$ T cells by administering antibodies specific for CD4 from day -2 to 14 dpi **(Fig. 5D-E)**. At 14 dpi, we harvested the lungs for enumeration of *M. tuberculosis* burden and neutrophil abundance and found that there was no effect of CD4$^+$ T cell depletion on either readout **(Fig. 5F-G)**. In addition, blocking IL-17A signaling by administering an anti-IL-17A antibody from day -1 to 14 dpi **(Fig. 5H)** did not affect *M. tuberculosis* burden **(Fig. 5I)** or neutrophil abundance **(Fig. 5J)** in *Atg5$^{fl/fl}$-LysM-Cre* mice and *Atg5$^{fl/fl}$* mice at 14 dpi. Therefore, although ATG5 is required in innate immune cells to suppress IL-17A expression in T cells, this role does not contribute to differences in neutrophil accumulation early during *M. tuberculosis* infection.

DISCUSSION

Atg5$^{fl/fl}$-LysM-Cre mice are extremely susceptible to *M. tuberculosis* infection, where neutrophils accumulate in the lungs of infected *Atg5$^{fl/fl}$-LysM-Cre* mice by 14 dpi and are sustained at high levels until the mice succumb to the infection between 30-40 dpi (3). It was previously unknown how ATG5 imparted control of neutrophil recruitment to the lungs during *M. tuberculosis* infection. We have discovered that ATG5 is required in CD11c^{+} lung macrophages and DCs to regulate proinflammatory cytokine production and neutrophil influx during *M. tuberculosis* infection. This role for ATG5 is shared with ATG16L1 and BECLIN 1, but not RUBICON, suggesting it is autophagy dependent and does not involve LAP. We were able to reproduce the heightened proinflammatory responses in *M. tuberculosis* infected autophagy-deficient BMDMs *in vitro*, suggesting that autophagy specifically suppresses inflammatory responses from macrophages during *M. tuberculosis* infection, although this does not rule out a similar role in DCs *in vivo*. Alveolar macrophages are among the first cells to encounter *M. tuberculosis* in the airways and orchestrate the initial response to infection, recruiting other innate immune cells to the lung (35, 36). We postulate that similar to the BMDMs, autophagy-deficient alveolar macrophages overproduce pro-inflammatory signals during *M. tuberculosis* infection, leading to increased neutrophil recruitment.

The increased levels of cytokines and chemokines produced by autophagy-deficient macrophages was dependent on *M. tuberculosis* infection, demonstrating that pathogen detection was required. However, the heightened proinflammatory responses in autophagy-deficient macrophages occurred in the absence of differences in bacterial burden, indicating that the enhanced inflammatory response is not due to increased antigen. In addition, the observation that loss of autophagy in macrophages *in vitro* or *in vivo* does not affect *M. tuberculosis* burden supports our prior findings that xenophagy is not required to control *M. tuberculosis* pathogenesis (3). Instead, our data supports a model where canonical autophagy is required in macrophages to control proinflammatory responses following *M. tuberculosis* infection. We ruled out the involvement of CASPASE1/11-dependent inflammasome activity and mitophagy in autophagy-dependent regulation of neutrophil accumulation during *M. tuberculosis* infection, leaving open the question of how autophagy regulates

macrophage proinflammatory responses during infection. One potential mechanism could involve the accumulation of damage associated signals in autophagy-deficient macrophages during infection. Release of damage associated molecular patterns (DAMPs) at sites of injury or infection activate endothelial cells to promote neutrophil adhesion and recruitment through cytokine and chemokine signaling (65). Sensing of DAMPs also activates autophagy to reduce inflammatory responses and cytokine production as well as clear cell debris (65, 66). Another possible mechanism for how autophagy regulates inflammatory responses from macrophages during *M. tuberculosis* infection involves the process of ER-phagy. ER-phagy is induced under conditions of ER stress, accumulation of unfolded proteins, and during infection (67, 68). ER-phagy restrains ER stress responses by targeting excess or damaged endoplasmic reticulum to autophagosomes for degradation (67), but in the absence of autophagy, ER stress activates NFκB-dependent transcription of inflammatory cytokines, such as IL-1β, IL-6, IL-18 and TNF-α (68).

We also discovered that ATG5 was required in innate immune cells to suppress early T_H17 responses during *M. tuberculosis* infection. The effect of loss of *Atg5* in innate immune cells on IL-17A expression from T cells may be explained by the requirement for autophagy in DCs to negatively regulate surface expression of disintegrin and metalloproteinase domain-containing protein 10 (ADAM10). ADAM10 cleaves its substrate ICOSL and lower levels of ICOSL leads to decreased ICOSL-ICOS interactions between DCs and T cells, resulting in less $CD25^{hi}$ $CD4^+$ T regulatory cells and more IL-17^+ $CD4^+$ T cells (69). In addition, autophagy negatively regulates T_H17 differentiation by reducing IL-23 and IL-1β levels, which promote T_H17 differentiation and IL-17A secretion (4, 70–72). Nonetheless, depleting $CD4^+$ T cells or blocking IL-17A did not rescue the increased neutrophil accumulation in the lungs of *M. tuberculosis* infected *Atg5$^{fl/fl}$-LysM-Cre* mice at 14 dpi, suggesting that the hyper-inflammatory responses from infected autophagy-deficient macrophages and DCs is sufficient to recruit excessive neutrophils early during infection. However, it is possible that the heightened T_H17 responses in *M. tuberculosis* infected *Atg5$^{fl/fl}$-LysM-Cre* mice have a longer-term impact on the increased susceptibility of these mice.

Our studies show that neutrophil recruitment to the lung early during *M. tuberculosis* infection is regulated in an autophagy-dependent manner, leaving open the question of what the autophagy-independent function for ATG5 is that has been shown to be required to control *M. tuberculosis* pathogenesis (3). At this point, we do not know if the increased abundance of IL-17^{+} CD4^{+} T cells in *M. tuberculosis* infected *Atg5$^{fl/fl}$-LysM-Cre* mice is due to an autophagy-dependent or independent role for ATG5. In addition, we have previously shown that loss of *Atg5* expression in neutrophils can result in earlier susceptibility than mice lacking the expression of other autophagy genes in neutrophils (3), suggesting that there is an autophagy-independent role for ATG5 in neutrophils that contributes to control of *M. tuberculosis* infection. We hypothesize that the combination of the newly discovered roles for autophagy in CD11c^{+} lung macrophages and DCs to regulate inflammatory responses and an autophagy-independent role for ATG5 in neutrophils collectively allow for control of *M. tuberculosis* infection, where loss of both functions results in the extreme susceptibility of *Atg5$^{fl/fl}$-LysM-Cre* mice to *M. tuberculosis* infection. Higher abundances of neutrophils have been associated with poor disease prognosis and treatment outcomes in TB patients (14–16). Therefore, our new findings and future dissection of the ATG5-dependent mechanisms of regulating neutrophil recruitment to the lungs during *M. tuberculosis* infection will provide critical insight into how to promote protective immune responses during TB.

ACKNOWLEDGEMENTS

The authors thank Dr. Jonathan Brestoff at Washington University School of Medicine for generously providing the *Parkin*$^{-/-}$ and *Pink1*$^{-/-}$ mice.

AUTHOR CONTRIBUTIONS

The experiments were designed by R.L.K., J.M.K., and C.L.S.. The experiments were executed by R.L.K., J.M.K., and A.S. with assistance from R.W., M.R.G. and S.M.C.. D.K. bred and maintained the mouse colonies. The manuscript was written by R.L.K. and C.L.S..

FIGURE LEGENDS

Figure 1. ATG5 is required in CD11c^{+} cells to regulate the early influx of neutrophils during *M. tuberculosis* infection *in vivo*. (A) Representative flow cytometry plots of neutrophils (CD45^{+}Ly6G^{+}CD11b^{+}) at 14 days post-infection (dpi) from *Atg5*$^{fl/fl}$, *Atg5*$^{fl/fl}$*-LysM-Cre*, *Atg5*$^{fl/fl}$*-CD11c-Cre* and *Atg5*$^{fl/fl}$*-Mrp8-Cre* mice. **(B)** Proportion of CD45^{+} cells that are neutrophils in the lung at 14 dpi in *Atg5*$^{fl/fl}$, *Atg5*$^{fl/fl}$*-LysM-Cre*, *Atg5*$^{fl/fl}$*-CD11c-Cre*, and *Atg5*$^{fl/fl}$*-Mrp8-Cre* mice. Neutrophil frequency is reported as a ratio relative to the average neutrophil frequency in *Atg5*$^{fl/fl}$ control mice at 14 dpi within a given experiment. **(C)** Lung burden from the right lung at 14 dpi in *Atg5*$^{fl/fl}$, *Atg5*$^{fl/fl}$*-LysM-Cre*, *Atg5*$^{fl/fl}$*-CD11c-Cre*, and *Atg5*$^{fl/fl}$*-Mrp8-Cre* mice. **(D)** Proportion of CD45^{+} cells that are neutrophils in the lung at 21 dpi in *Atg5*$^{fl/fl}$, *Atg5*$^{fl/fl}$*-LysM-Cre*, *Atg5*$^{fl/fl}$*-CD11c-Cre* and *Atg5*$^{fl/fl}$*-Mrp8-Cre* mice. Neutrophil frequency is reported as a ratio relative to the average neutrophil frequency in *Atg5*$^{fl/fl}$ control mice at 21 dpi within a given experiment. Sick and healthy *Atg5*$^{fl/fl}$*-Mrp8-Cre* mice are defined as done previously where sick *Atg5*$^{fl/fl}$*-Mrp8-Cre* mice have lost more than 30% of their pre-infection body weight by 21 dpi and healthy *Atg5*$^{fl/fl}$*-Mrp8-Cre* mice have lost less than 30% of their pre-infection body weight at 21 dpi (3). **(E)** Lung burden from the right lung at 21 dpi in *Atg5*$^{fl/fl}$, *Atg5*$^{fl/fl}$*-LysM-Cre*, *Atg5*$^{fl/fl}$*-CD11c-Cre*, and *Atg5*$^{fl/fl}$*-Mrp8-Cre* mice. **(F)** Kaplan Meier curve of survival proportions during *M. tuberculosis* infection of *Atg5*$^{fl/fl}$ and *Atg5*$^{fl/fl}$*-CD11c-Cre* mice. Statistical differences were determined by a log-rank Mantel-Cox test (F) or one-way ANOVA and Šídák multiple comparison test (B-E). * $P < 0.05$, ** $P < 0.01$, *** $P < 0.001$, **** $P < 0.0001$. Differences

that are not statistically significant are designated as ns. Each data point is from one biological replicate and at least two separate experiments were performed.

Figure 2. The role for ATG5 in macrophages and DCs in regulating neutrophil recruitment is dependent on other autophagy proteins. (A) Proportion of $CD45^+$ cells that are neutrophils ($CD45^+Ly6G^+CD11b^+$) in the lung at 14 dpi in *Becn1*$^{fl/fl}$ or *Becn1*$^{fl/fl}$*-CD11c-Cre* mice. Neutrophil frequency is reported as a ratio relative to the average neutrophil frequency in *Becn1*$^{fl/fl}$ control mice at 14 dpi. **(B)** Lung burden from the right lobes of the lung at 14 dpi in *Becn1*$^{fl/fl}$ or *Becn1*$^{fl/fl}$*-CD11c-Cre* mice. **(C)** Neutrophil frequency of $CD45^+$ cells reported as a ratio to the average neutrophil frequency in floxed control mice in *Atg5*$^{fl/fl}$, *Atg5*$^{fl/fl}$*-LysM-Cre*, *Becn1*$^{fl/fl}$, *Becn1*$^{fl/fl}$*-LysM-Cre*, *Atg16l1*$^{fl/fl}$, *Atg16l1*$^{fl/fl}$*-LysM-Cre* mice. Neutrophil frequencies in *Rubicon*$^{-/-}$ mice were compared to wildtype C57BL/6J mice. **(D)** Lung burden from right lobes of the lung at 14 dpi in *Atg5*$^{fl/fl}$, *Atg5*$^{fl/fl}$*-LysM-Cre*, *Becn1*$^{fl/fl}$, *Becn1*$^{fl/fl}$*-LysM-Cre*, *Atg16l1*$^{fl/fl}$, *Atg16l1*$^{fl/fl}$*-LysM-Cre*, wildtype C57BL/6J, and *Rubicon*$^{-/-}$ mice. Statistical differences were determined by student t-test to compare the Cre expressing mice to their respective floxed control and *Rubicon*$^{-/-}$ mice to wildtype C57BL/6J mice (A-D). * $P < 0.05$, ** $P < 0.01$, *** $P < 0.001$, **** $P < 0.0001$. Differences that are not statistically significant are designated as ns. Each data point is from one biological replicate and at least two separate experiments were performed.

Figure 3. Autophagy regulates proinflammatory responses in macrophages during *M. tuberculosis* infection. (A) Cytokine bead array data to quantify cytokines in culture supernatants from *Atg5*$^{fl/fl}$, *Atg5*$^{fl/fl}$*-LysM-Cre*$^-$, *Atg16l1*$^{fl/fl}$, *Atg16l1*$^{fl/fl}$*-LysM-Cre*, *Becn1*$^{fl/fl}$ or *Becn1*$^{fl/fl}$*-LysM-Cre* BMDMs mock-treated or infected with *M. tuberculosis* at an MOI of 10 for 24 hours. BMDMs generated from at least 3 mice were tested in duplicate to quantify cytokine production. **(A)** IL-1β, **(B)** G-CSF, **(C)** IL-6, **(D)** KC, and **(E)** TNF-α, and **(F)** RANTES levels at 24 hpi are shown. **(G)** BMDM CFU counts at 24 hpi. **(H)** KC, **(I)** G-CSF, and **(J)** IL-6 levels at 24 hpi in *Atg5*$^{fl/fl}$ and *Atg5*$^{-/-}$ BMDMs infected with *M. tuberculosis* at an MOI of 10 or 20 for 24 hours determined by ELISA. Statistical differences were determined by student t-test to compare the autophagy gene-deficient cells to their

493 respective floxed control cells (A-J). * P < 0.05, ** P < 0.01, *** P < 0.001, **** P < 0.0001. Differences that
494 are not statistically significant are designated as ns. Cytokine levels below detection limits are designated as bdl.
495 Each data point is one biological replicate.
496
497 **Figure 4. Autophagy suppresses neutrophil recruitment independent of mitophagy and inflammasome**
498 **activation during *M. tuberculosis* infection. (A)** Proportion of $CD45^+$ cells that are neutrophils
499 ($CD45^+Ly6G^+CD11b^+$) in the lung at 14 dpi in *Becn1*$^{fl/fl}$, *Becn1*$^{fl/fl}$*-LysM-Cre*, *Caspase1/11*$^{-/-}$*/Becn1*$^{fl/fl}$,
500 *Caspase1/11*$^{-/-}$*/Becn1*$^{fl/fl}$*-LysM-Cre*, *Atg5*$^{fl/fl}$, *Atg5*$^{fl/fl}$*-LysM-Cre*, *Caspase1/11*$^{-/-}$*/Atg5*$^{fl/fl}$, or *Caspase1/11*$^{-/-}$*/Atg5*$^{fl/fl}$-
501 *LysM-Cre* mice reported as a ratio relative to the average neutrophil frequency in corresponding floxed control
502 mice. **(B)** Lung burden at 14 dpi from right lobes of the lung from *Becn1*$^{fl/fl}$, *Becn1*$^{fl/fl}$*-LysM-Cre*, *Caspase1/11*$^{-/-}$
503 */Becn1*$^{fl/fl}$, *Caspase1/11*$^{-/-}$*/Becn1*$^{fl/fl}$*-LysM-Cre*, *Atg5*$^{fl/fl}$, *Atg5*$^{fl/fl}$*-LysM-Cre*, *Caspase1/11*$^{-/-}$*/Atg5*$^{fl/fl}$, or
504 *Caspase1/11*$^{-/-}$*/Atg5*$^{fl/fl}$*-LysM-Cre* mice. The legend in 4A also applies to 4B. **(C)** Kaplan Meier curve of survival
505 proportions during *M. tuberculosis* infection of *Atg5*$^{fl/fl}$, *Atg5*$^{fl/fl}$*-LysM-Cre*, *Caspase1/11*$^{-/-}$*/Atg5*$^{fl/fl}$, and
506 *Caspase1/11*$^{-/-}$*/Atg5*$^{fl/fl}$*-LysM-Cre* mice. **(D)** Proportion of $CD45^+$ cells that are neutrophils
507 ($CD45^+Ly6G^+CD11b^+$) in the lung at 14 dpi in wildtype, *Parkin*$^{-/-}$, and *Pink1*$^{-/-}$ mice reported as a ratio relative
508 to the average neutrophil frequency in wildtype C57BL/6J mice. **(E)** Lung burden from the right lobe of the lung
509 at 14 dpi in wildtype C57BL/6J, *Parkin*$^{-/-}$, and *Pink1*$^{-/-}$ mice. Statistical differences were determined by log-rank
510 Mantel-Cox test (C) and one-way ANOVA and Šídák multiple comparison test (A-B, D-E). * P < 0.05, ** P <
511 0.01, *** P < 0.001, **** P < 0.0001. Differences that are not statistically significant are designated as ns. Each
512 data point is from one biological replicate and at least two separate experiments were performed.
513
514 **Figure 5. ATG5 is required to suppress early T_H17 responses during *M. tuberculosis* infection. (A)** The
515 number of $CD4^+$ T cells ($CD45^+$ $TCR\beta^+$ $CD4^+$) in *Atg5*$^{fl/fl}$ and *Atg5*$^{fl/fl}$*-LysM-Cre* mice are reported as the total
516 cells per lung in the left lobe at 14 dpi. **(B)** The frequency of IL-17-GFP^+ $CD4^+$ T cells in the lung ($CD45^+$ $TCR\beta^+$
517 $CD4^+$ IL-17-GFP^+) of *Atg5*$^{fl/fl}$ and *Atg5*$^{fl/fl}$*-LysM-Cre* mice are reported as the percentage of $CD4^+$ T cells that are

IL-17-GFP positive at 14 dpi. **(C)** The number IL-17-GFP$^+$ CD4$^+$ T cells in *Atg5$^{fl/fl}$* and *Atg5$^{fl/fl}$-LysM-Cre* mice are reported as the total cells per lung in the left lobe at 14 dpi. **(D)** Schematic depicting the timing of CD4 antibody injections. **(E)** The number of CD4$^+$ T cells (CD45$^+$ TCRβ$^+$ CD4$^+$) in *Atg5$^{fl/fl}$* and *Atg5$^{fl/fl}$-LysM-Cre* mice are reported as the total cells per lung in the left lobe at 14 dpi following antibody treatment. **(F)** Lung burden from the right lobes of the lung at 14 dpi in *Atg5$^{fl/fl}$* or *Atg5$^{fl/fl}$-LysM-Cre* mice that received isotype or CD4-depletion antibodies. **(G)** Proportion of CD45$^+$ cells that are neutrophils (CD45$^+$Ly6G$^+$CD11b$^+$) in the lung at 14 dpi in *Atg5$^{fl/fl}$* or *Atg5$^{fl/fl}$-LysM-Cre* mice that received CD4 antibody or an isotype control. Neutrophil frequency is reported as a ratio relative to the average neutrophil frequency in *Atg5$^{fl/fl}$* control mice at 14 dpi. **(H)** Schematic depicting delivery of the IL-17 neutralizing antibody treatments. **(I)** Lung burden from the right lobes of the lung at 14 dpi in *Atg5$^{fl/fl}$* or *Atg5$^{fl/fl}$-LysM-Cre* mice that received isotype or IL-17 neutralizing antibodies. **(J)** Proportion of CD45$^+$ cells that are neutrophils (CD45$^+$Ly6G$^+$CD11b$^+$) in the lung at 14 dpi in *Atg5$^{fl/fl}$* or *Atg5$^{fl/fl}$-LysM-Cre* mice that received isotype or IL-17 neutralizing antibodies. Neutrophil frequency is reported as a ratio relative to the average neutrophil frequency in *Atg5$^{fl/fl}$* control mice at 14 dpi. Statistical differences were determined by student t-test (A) or one-way ANOVA and Šídák multiple comparison test (A-C, E-G, I and J). * $P < 0.05$, ** $P < 0.01$, *** $P < 0.001$, **** $P < 0.0001$. Differences that are not statistically significant are designated as ns. Each data point is from one biological replicate.

Supplemental Figure 1. Gating strategies for flow cytometry identification of neutrophils and IL-17A expressing T cells. (A) Cells from the lung were identified as viable by not staining with Zombie-NIR, hematopoietic cells were identified as CD45$^+$ and neutrophils were identified as Ly6G$^+$ and CD11b$^+$. **(B)** T_H17 cells were identified in *Il17a-GFP/Atg5$^{fl/fl}$* and *Il17a-GFP/Atg5$^{fl/fl}$-LysM-Cre* mice by gating viable cells based on not staining with Zombie-NIR, hematopoietic cells were identified as CD45$^+$, all non-neutrophils were identified as Ly6G$^-$, and CD4$^+$ T cells were identified as TCRβ$^+$, CD19$^-$, and CD4$^+$. IL-17 expressing T cells were gated as IL-17-GFP$^+$ CD4$^+$ T cells.

Supplemental Figure 2. Levels of cytokines and chemokines that were not significantly different in ATG5-deficient macrophages. Cytokine bead array data from mock treated and *M. tuberculosis* infected BMDMs. *Atg5$^{fl/fl}$*, *Atg5$^{fl/fl}$-LysM-Cre*, *Atg16l1$^{fl/fl}$*, *Atg16l1$^{fl/fl}$-LysM-Cre*, *Becn1$^{fl/fl}$* and *Becn1$^{fl/fl}$-LysM-Cre* BMDMs were cultured for 24 hpi and cytokine levels were measured in the media from mock treated or infected macrophages. BMDMs from at least 3 mice were tested in duplicate to quantify the cytokines in the bead array. All cytokine and chemokine data that are not significantly different between macrophages cultured from *Atg5$^{fl/fl}$-LysM-Cre* and *Atg5$^{fl/fl}$* mice are reported here. **(A)** IL-1α, **(B)** IL-3, **(C)** IL-4, **(D)** IL-5, **(E)** IL-10, **(F)** IL-12(p40), **(G)** IL-12(p70), **(H)** IFN-γ, **(I)** MIP1β, **(J)** GM-CSF, **(K)** MIP1α, **(L)** MCP-1, **(M)** Eotaxin, and **(N)** IL-17 levels at 24 hpi. Statistical differences were determined by student t-test comparing the autophagy deficient macrophage with its floxed control within a treatment condition (A-N). * $P < 0.05$, ** $P < 0.01$, *** $P < 0.001$, **** $P < 0.0001$. Cytokine levels below detection limits are designated as bdl. Differences that are not statistically significant are designated as ns.

Supplemental Figure 3. Mitophagy is not required in macrophages to regulate proinflammatory responses during *M. tuberculosis* infection. WT, *Parkin$^{-/-}$* and *Pink1$^{-/-}$*, BMDMs were cultured for 24 hpi and cytokine levels were measured by cytokine bead array in the media from mock treated or infected macrophages. **(A)** IL-1β levels at 24 hpi. **(B)** G-CSF levels at 24 hpi. **(C)** IL-6 levels at 24 hpi. **(D)** KC levels at 24 hpi. **(E)** RANTES levels at 24 hpi. **(F)** TNF-α levels at 24 hpi. **(G)** BMDM CFU counts at 24 hpi. BMDMs from at least 3 mice were tested in duplicate to quantify the cytokines in the bead array. Each point is one biological replicate. Statistical differences were determined by one-way ANOVA and Šídák multiple comparison test (A-G). * $P < 0.05$, ** $P < 0.01$, *** $P < 0.001$, **** $P < 0.0001$. Cytokine levels below detection limits are designated as dbl. Statistical differences that are not significant are designated as ns.

REFERENCES

1. World Health Organization. Regional Office for South-East Asia. 2022. *WHO global Tuberculosis report 2021,*. World Health Organization. Regional Office for South-East Asia, New Delhi.

2. Kinsella, R., D. Zhu, G. Harrison, A. Mayer Bridwell, J. Prusa, S. Chavez, and C. Stallings. 2021. Perspectives and Advances in the Understanding of Tuberculosis. *Annu Rev Pathol.* 16: 377–408.

3. Kimmey, J. M., J. P. Huynh, L. A. Weiss, S. Park, A. Kambal, J. Debnath, H. W. Virgin, and C. L. Stallings. 2015. Unique role for ATG5 in neutrophil-mediated immunopathology during M. tuberculosis infection. *Nature* 528: 565–569.

4. Castillo, E. F., A. Dekonenko, J. Arko-Mensah, M. A. Mandell, N. Dupont, S. Jiang, M. Delgado-Vargas, G. S. Timmins, D. Bhattacharya, H. Yang, J. Hutt, C. R. Lyons, K. M. Dobos, and V. Deretic. 2012. Autophagy protects against active tuberculosis by suppressing bacterial burden and inflammation. *Proc. Natl. Acad. Sci.* 109: E3168–E3176.

5. Watson, R. O., P. S. Manzanillo, and J. S. Cox. 2012. Extracellular M. tuberculosis DNA Targets Bacteria for Autophagy by Activating the Host DNA-Sensing Pathway. *Cell* 150: 803–815.

6. Mishra, B. B., R. R. Lovewell, A. J. Olive, G. Zhang, W. Wang, E. Eugenin, C. M. Smith, J. Y. Phuah, J. E. Long, M. L. Dubuke, S. G. Palace, J. D. Goguen, R. E. Baker, S. Nambi, R. Mishra, M. G. Booty, C. E. Baer, S. A. Shaffer, V. Dartois, B. A. McCormick, X. Chen, and C. M. Sassetti. 2017. Nitric oxide prevents a pathogen-permissive granulocytic inflammation during tuberculosis. *Nat. Microbiol.* 2: 17072.

7. Mishra, B. B., V. A. K. Rathinam, G. W. Martens, A. J. Martinot, H. Kornfeld, K. A. Fitzgerald, and C. M. Sassetti. 2013. Nitric oxide controls the immunopathology of tuberculosis by inhibiting NLRP3 inflammasome–dependent processing of IL-1β. *Nat. Immunol.* 14: 52–60.

8. Nandi, B., and S. M. Behar. 2011. Regulation of neutrophils by interferon-γ limits lung inflammation during tuberculosis infection. *J. Exp. Med.* 208: 2251–2262.

9. Niazi, M. K. K., N. Dhulekar, D. Schmidt, S. Major, R. Cooper, C. Abeijon, D. Gatti, I. Kramnik, B. Yener, M. Gurcan, and G. Beamer. 2015. Lung necrosis and neutrophils reflect common pathways of susceptibility to *Mycobacterium tuberculosis* in genetically diverse, immune competent mice. *Dis. Model. Mech.* dmm.020867.

10. Nair, S., J. P. Huynh, V. Lampropoulou, E. Loginicheva, E. Esaulova, A. P. Gounder, A. C. M. Boon, E. A. Schwarzkopf, T. R. Bradstreet, B. T. Edelson, M. N. Artyomov, C. L. Stallings, and M. S. Diamond. 2018. Irg1 expression in myeloid cells prevents immunopathology during M. tuberculosis infection. *J. Exp. Med.* 215: 1035–1045.

11. Dorhoi, A., V. Yeremeev, G. Nouailles, J. Weiner, S. Jörg, E. Heinemann, D. Oberbeck-Müller, J. K. Knaul, A. Vogelzang, S. T. Reece, K. Hahnke, H. Mollenkopf, V. Brinkmann, and S. H. E. Kaufmann. 2014. Type I IFN signaling triggers immunopathology in tuberculosis-susceptible mice by modulating lung phagocyte dynamics. *Eur. J. Immunol.* 44: 2380–2393.

12. Moreira-Teixeira, L., P. J. Stimpson, E. Stavropoulos, S. Hadebe, P. Chakravarty, M. Ioannou, I. V. Aramburu, E. Herbert, S. L. Priestnall, A. Suarez-Bonnet, J. Sousa, K. L. Fonseca, Q. Wang, S. Vashakidze, P. Rodríguez-Martínez, C. Vilaplana, M. Saraiva, V. Papayannopoulos, and A. O'Garra. 2020. Type I IFN exacerbates disease in tuberculosis-susceptible mice by inducing neutrophil-mediated lung inflammation and NETosis. *Nat. Commun.* 11: 5566.

13. Moreira-Teixeira, L., O. Tabone, C. M. Graham, A. Singhania, E. Stavropoulos, P. S. Redford, P. Chakravarty, S. L. Priestnall, A. Suarez-Bonnet, E. Herbert, K. D. Mayer-Barber, A. Sher, K. L. Fonseca, J. Sousa, B. Cá, R. Verma, P. Haldar, M. Saraiva, and A. O'Garra. 2020. Mouse transcriptome reveals potential signatures of protection and pathogenesis in human tuberculosis. *Nat. Immunol.* 21: 464–476.

14. Carvalho, A. C. C., G. Amorim, M. G. M. Melo, A. K. A. Silveira, P. H. L. Vargas, A. S. R. Moreira, M. S. Rocha, A. B. Souza, M. B. Arriaga, M. Araújo-Pereira, M. C. Figueiredo, B. Durovni, J. R. Lapa-e-Silva, S. Cavalcante, V. C. Rolla, T. R. Sterling, M. Cordeiro-Santos, B. B. Andrade, E. C. Silva, A. L. Kritski, and the RePORT Brazil consortium. 2021. Pre-Treatment Neutrophil Count as a Predictor of Antituberculosis Therapy Outcomes: A Multicenter Prospective Cohort Study. *Front. Immunol.* 12: 661934.

15. Han, Y., S. J. Kim, S. H. Lee, Y. S. Sim, Y. J. Ryu, J. H. Chang, S. S. Shim, Y. Kim, and J. H. Lee. 2018. High blood neutrophil-lymphocyte ratio associated with poor outcomes in miliary tuberculosis. *J. Thorac. Dis.* 10: 339–346.

16. Lowe, D. M., A. K. Bandara, G. E. Packe, R. D. Barker, R. J. Wilkinson, C. J. Griffiths, and A. R. Martineau. 2013. Neutrophilia independently predicts death in tuberculosis: Table 1–. *Eur. Respir. J.* 42: 1752–1757.

17. Berry, M. P. R., C. M. Graham, F. W. McNab, Z. Xu, S. A. A. Bloch, T. Oni, K. A. Wilkinson, R. Banchereau, J. Skinner, R. J. Wilkinson, C. Quinn, D. Blankenship, R. Dhawan, J. J. Cush, A. Mejias, O. Ramilo, O. M. Kon, V. Pascual, J. Banchereau, D. Chaussabel, and A. O'Garra. 2010. An interferon-inducible neutrophil-driven blood transcriptional signature in human tuberculosis. *Nature* 466: 973–977.

18. Kinsella, R. L., E. M. Nehls, and C. L. Stallings. 2018. Roles for Autophagy Proteins in Immunity and Host Defense. *Vet. Pathol.* 55: 366–373.

19. Kimmey, J. M., and C. L. Stallings. 2016. Bacterial Pathogens versus Autophagy: Implications for Therapeutic Interventions. *Trends Mol. Med.* 22: 1060–1076.

20. Lamb, C. A., T. Yoshimori, and S. A. Tooze. 2013. The autophagosome: origins unknown, biogenesis complex. *Nat. Rev. Mol. Cell Biol.* 14: 759–774.

21. Mizushima, N., T. Yoshimori, and Y. Ohsumi. 2011. The Role of Atg Proteins in Autophagosome Formation. *Annu. Rev. Cell Dev. Biol.* 27: 107–132.

22. Mizushima, N., T. Noda, T. Yoshimori, Y. Tanaka, T. Ishii, M. D. George, D. J. Klionsky, M. Ohsumi, and Y. Ohsumi. 1998. A protein conjugation system essential for autophagy. *Nature* 395: 395–398.

23. Wang, Y.-T., K. Zaitsev, Q. Lu, S. Li, W. T. Schaiff, K.-W. Kim, L. Droit, C. B. Wilen, C. Desai, D. R. Balce, R. C. Orchard, A. Orvedahl, S. Park, D. Kreamalmeyer, S. A. Handley, J. D. Pfeifer, M. T. Baldridge, M. N. Artyomov, C. L. Stallings, and H. W. Virgin. 2020. Select autophagy genes maintain quiescence of tissue-resident macrophages and increase susceptibility to Listeria monocytogenes. *Nat. Microbiol.* 5: 272–281.

24. Wang, Y.-T., A. Sansone, A. Smirnov, C. L. Stallings, and A. Orvedahl. 2022. Myeloid autophagy genes protect mice against fatal TNF- and LPS-induced cytokine storm syndromes. *Autophagy* 1–14.

25. Martinez, J., R. K. S. Malireddi, Q. Lu, L. D. Cunha, S. Pelletier, S. Gingras, R. Orchard, J.-L. Guan, H. Tan, J. Peng, T.-D. Kanneganti, H. W. Virgin, and D. R. Green. 2015. Molecular characterization of LC3-associated phagocytosis reveals distinct roles for Rubicon, NOX2 and autophagy proteins. *Nat. Cell Biol.* 17: 893–906.

26. Kitada, T., A. Pisani, D. R. Porter, H. Yamaguchi, A. Tscherter, G. Martella, P. Bonsi, C. Zhang, E. N. Pothos, and J. Shen. 2007. Impaired dopamine release and synaptic plasticity in the striatum of *PINK1* -deficient mice. *Proc. Natl. Acad. Sci.* 104: 11441–11446.

27. Goldberg, M. S., S. M. Fleming, J. J. Palacino, C. Cepeda, H. A. Lam, A. Bhatnagar, E. G. Meloni, N. Wu, L. C. Ackerson, G. J. Klapstein, M. Gajendiran, B. L. Roth, M.-F. Chesselet, N. T. Maidment, M. S. Levine, and J. Shen. 2003. Parkin-deficient Mice Exhibit Nigrostriatal Deficits but Not Loss of Dopaminergic Neurons. *J. Biol. Chem.* 278: 43628–43635.

28. Huynh, J. P., C.-C. Lin, J. M. Kimmey, N. N. Jarjour, E. A. Schwarzkopf, T. R. Bradstreet, I. Shchukina, O. Shpynov, C. T. Weaver, R. Taneja, M. N. Artyomov, B. T. Edelson, and C. L. Stallings. 2018. Bhlhe40 is an essential repressor of IL-10 during Mycobacterium tuberculosis infection. *J. Exp. Med.* 215: 1823–1838.

29. Domingo-Gonzalez, R., S. Das, K. L. Griffiths, M. Ahmed, M. Bambouskova, R. Gopal, S. Gondi, M. Muñoz-Torrico, M. A. Salazar-Lezama, A. Cruz-Lagunas, L. Jiménez-Álvarez, G. Ramirez-Martinez, R. Espinosa-Soto, T. Sultana, J. Lyons-Weiler, T. A. Reinhart, J. Arcos, M. de la Luz Garcia-Hernandez, M. A. Mastrangelo, N. Al-Hammadi, R. Townsend, J.-M. Balada-Llasat, J. B. Torrelles, G. Kaplan, W. Horne, J. K. Kolls, M. N. Artyomov, J. Rangel-Moreno, J. Zúñiga, and S. A. Khader. 2017. Interleukin-17 limits hypoxia-inducible factor 1α and development of hypoxic granulomas during tuberculosis. *JCI Insight* 2: e92973.

30. Martinez, J., L. D. Cunha, S. Park, M. Yang, Q. Lu, R. Orchard, Q.-Z. Li, M. Yan, L. Janke, C. Guy, A. Linkermann, H. W. Virgin, and D. R. Green. 2016. Noncanonical autophagy inhibits the autoinflammatory, lupus-like response to dying cells. *Nature* 533: 115–119.

31. Heckmann, B. L., and D. R. Green. 2019. LC3-associated phagocytosis at a glance. *J. Cell Sci.* 132: jcs231472.

32. Wan, J., E. Weiss, S. Ben Mkaddem, M. Mabire, P.-M. Choinier, O. Picq, T. Thibault-Sogorb, P. Hegde, D. Pishvaie, M. Bens, L. Broer, H. Gilgenkrantz, R. Moreau, L. Saveanu, P. Codogno, R. C. Monteiro, and S. Lotersztajn. 2020. LC3-associated phagocytosis protects against inflammation and liver fibrosis via immunoreceptor inhibitory signaling. *Sci. Transl. Med.* 12: eaaw8523.

33. Sanjuan, M. A., C. P. Dillon, S. W. G. Tait, S. Moshiach, F. Dorsey, S. Connell, M. Komatsu, K. Tanaka, J. L. Cleveland, S. Withoff, and D. R. Green. 2007. Toll-like receptor signalling in macrophages links the autophagy pathway to phagocytosis. *Nature* 450: 1253–1257.

34. Martinez, J., J. Almendinger, A. Oberst, R. Ness, C. P. Dillon, P. Fitzgerald, M. O. Hengartner, and D. R. Green. 2011. Microtubule-associated protein 1 light chain 3 alpha (LC3)-associated phagocytosis is required for the efficient clearance of dead cells. *Proc. Natl. Acad. Sci.* 108: 17396–17401.

35. Cohen, S. B., B. H. Gern, J. L. Delahaye, K. N. Adams, C. R. Plumlee, J. K. Winkler, D. R. Sherman, M. Y. Gerner, and K. B. Urdahl. 2018. Alveolar Macrophages Provide an Early Mycobacterium tuberculosis Niche and Initiate Dissemination. *Cell Host Microbe* 24: 439-446.e4.

36. Rothchild, A. C., G. S. Olson, J. Nemeth, L. M. Amon, D. Mai, E. S. Gold, A. H. Diercks, and A. Aderem. 2019. Alveolar macrophages generate a noncanonical NRF2-driven transcriptional response *to Mycobacterium tuberculosis* in vivo. *Sci. Immunol.* 4: eaaw6693.

37. Vieira, S., H. Lemos, R. Grespan, M. Napimoga, D. Dal-Secco, A. Freitas, T. Cunha, W. V. Jr, D. Souza-Junior, M. Jamur, K. Fernandes, C. Oliver, J. Silva, M. Teixeira, and F. Cunha. 2009. A crucial role for TNF-a in mediating neutrophil influx induced by endogenously generated or exogenous chemokines, KC/CXCL1 and LIX/CXCL5. *Br. J. Pharmacol.* 11.

38. Bendall, L. J., and K. F. Bradstock. 2014. G-CSF: From granulopoietic stimulant to bone marrow stem cell mobilizing agent. *Cytokine Growth Factor Rev.* 25: 355–367.

39. Semerad, C. L., F. Liu, A. D. Gregory, K. Stumpf, and D. C. Link. 2002. G-CSF Is an Essential Regulator of Neutrophil Trafficking from the Bone Marrow to the Blood. *Immunity* 17: 413–423.

40. Pollara, G., C. T. Turner, J. Rosenheim, A. Chandran, L. C. K. Bell, A. Khan, A. Patel, L. F. Peralta, A. Folino, A. Akarca, C. Venturini, T. Baker, S. Ecker, F. L. M. Ricciardolo, T. Marafioti, C. Ugarte-Gil, D. A. J. Moore, B. M. Chain, G. S. Tomlinson, and M. Noursadeghi. 2021. Exaggerated IL-17A activity in human in vivo recall responses discriminates active tuberculosis from latent infection and cured disease. *Sci. Transl. Med.* 13: eabg7673.

41. Sasaki, Y., Y.-M. Guo, T. Goto, K. Ubukawa, K. Asanuma, I. Kobayashi, K. Sawada, H. Wakui, and N. Takahashi. 2021. IL-6 Generated from Human Hematopoietic Stem and Progenitor Cells through TLR4 Signaling Promotes Emergency Granulopoiesis by Regulating Transcription Factor Expression. *J. Immunol.* ji2100168.

42. Hu, S., W. He, X. Du, J. Yang, Q. Wen, X.-P. Zhong, and L. Ma. 2017. IL-17 Production of Neutrophils Enhances Antibacteria Ability but Promotes Arthritis Development During Mycobacterium tuberculosis Infection. *EBioMedicine* 23: 88–99.

43. Fielding, C. A., R. M. McLoughlin, L. McLeod, C. S. Colmont, M. Najdovska, D. Grail, M. Ernst, S. A. Jones, N. Topley, and B. J. Jenkins. 2008. IL-6 Regulates Neutrophil Trafficking during Acute Inflammation via STAT3. *J. Immunol.* 181: 2189–2195.

44. Saitoh, T., and S. Akira. 2016. Regulation of inflammasomes by autophagy. *J. Allergy Clin. Immunol.* 138: 28–36.

45. Harris, J., M. Hartman, C. Roche, S. G. Zeng, A. O'Shea, F. A. Sharp, E. M. Lambe, E. M. Creagh, D. T. Golenbock, J. Tschopp, H. Kornfeld, K. A. Fitzgerald, and E. C. Lavelle. 2011. Autophagy Controls IL-1β Secretion by Targeting Pro-IL-1β for Degradation. *J. Biol. Chem.* 286: 9587–9597.

46. Ko, J. H., S.-O. Yoon, H. J. Lee, and J. Y. Oh. 2017. Rapamycin regulates macrophage activation by inhibiting NLRP3 inflammasome-p38 MAPK-NFκB pathways in autophagy- and p62-dependent manners. *Oncotarget* 8: 40817–40831.

47. Shi, C.-S., K. Shenderov, N.-N. Huang, J. Kabat, M. Abu-Asab, K. A. Fitzgerald, A. Sher, and J. H. Kehrl. 2012. Activation of autophagy by inflammatory signals limits IL-1β production by targeting ubiquitinated inflammasomes for destruction. *Nat. Immunol.* 13: 255–263.

48. Pyrillou, K., L. C. Burzynski, and M. C. H. Clarke. 2020. Alternative Pathways of IL-1 Activation, and Its Role in Health and Disease. *Front. Immunol.* 11: 613170.

49. McElvania TeKippe, E., I. C. Allen, P. D. Hulseberg, J. T. Sullivan, J. R. McCann, M. Sandor, M. Braunstein, and J. P.-Y. Ting. 2010. Granuloma Formation and Host Defense in Chronic Mycobacterium tuberculosis Infection Requires PYCARD/ASC but Not NLRP3 or Caspase-1. *PLoS ONE* 5: e12320.

50. Beckwith, K. S., M. S. Beckwith, S. Ullmann, R. S. Sætra, H. Kim, A. Marstad, S. E. Åsberg, T. A. Strand, M. Haug, M. Niederweis, H. A. Stenmark, and T. H. Flo. 2020. Plasma membrane damage causes NLRP3 activation and pyroptosis during Mycobacterium tuberculosis infection. *Nat. Commun.* 11: 2270.

51. Abdalla, H., L. Srinivasan, S. Shah, K. D. Mayer-Barber, A. Sher, F. S. Sutterwala, and V. Briken. 2012. Mycobacterium tuberculosis Infection of Dendritic Cells Leads to Partially Caspase-1/11-Independent IL-1β and IL-18 Secretion but Not to Pyroptosis. *PLoS ONE* 7: e40722.

52. Mayer-Barber, K. D., D. L. Barber, K. Shenderov, S. D. White, M. S. Wilson, A. Cheever, D. Kugler, S. Hieny, P. Caspar, G. Núñez, D. Schlueter, R. A. Flavell, F. S. Sutterwala, and A. Sher. 2010. Cutting Edge: Caspase-1 Independent IL-1β Production Is Critical for Host Resistance to *Mycobacterium tuberculosis* and Does Not Require TLR Signaling In Vivo. *J. Immunol.* 184: 3326–3330.

53. Lin, K.-M., W. Hu, T. D. Troutman, M. Jennings, T. Brewer, X. Li, S. Nanda, P. Cohen, J. A. Thomas, and C. Pasare. 2014. IRAK-1 bypasses priming and directly links TLRs to rapid NLRP3 inflammasome activation. *Proc. Natl. Acad. Sci.* 111: 775–780.

54. Yu Qiao,Peng Wang,Jianni Qi,Lei Zhang,Chengjiang Gao. 1016. TLR-induced NF-jB activation regulates NLRP3 expression in murine macrophages. 2012: 1022–1026.

55. Lazarou, M., D. A. Sliter, L. A. Kane, S. A. Sarraf, C. Wang, J. L. Burman, D. P. Sideris, A. I. Fogel, and R. J. Youle. 2015. The ubiquitin kinase PINK1 recruits autophagy receptors to induce mitophagy. *Nature* 524: 309–314.

56. Killackey, S. A., D. J. Philpott, and S. E. Girardin. 2020. Mitophagy pathways in health and disease. *J. Cell Biol.* 219: e202004029.

57. Zhang, W., H. Ren, C. Xu, C. Zhu, H. Wu, D. Liu, J. Wang, L. Liu, W. Li, Q. Ma, L. Du, M. Zheng, C. Zhang, J. Liu, and Q. Chen. 2016. Hypoxic mitophagy regulates mitochondrial quality and platelet activation and determines severity of I/R heart injury. *eLife* 5: e21407.

58. Wang, S., S. M. Martin, P. S. Harris, and C. M. Knudson. 2011. Caspase Inhibition Blocks Cell Death and Enhances Mitophagy but Fails to Promote T-Cell Lymphoma. *PLoS ONE* 6: e19786.

59. Nguyen, T. N., B. S. Padman, and M. Lazarou. 2016. Deciphering the Molecular Signals of PINK1/Parkin Mitophagy. *Trends Cell Biol.* 26: 733–744.

60. Harris, J., N. Deen, S. Zamani, and M. A. Hasnat. 2018. Mitophagy and the release of inflammatory cytokines. *Mitochondrion* 41: 2–8.

61. Song, Y., Y. Zhou, and X. Zhou. 2020. The role of mitophagy in innate immune responses triggered by mitochondrial stress. *Cell Commun. Signal.* 18: 186.

62. Griffin, G. K., G. Newton, M. L. Tarrio, D. Bu, E. Maganto-Garcia, V. Azcutia, P. Alcaide, N. Grabie, F. W. Luscinskas, K. J. Croce, and A. H. Lichtman. 2012. IL-17 and TNF-α Sustain Neutrophil Recruitment during Inflammation through Synergistic Effects on Endothelial Activation. *J. Immunol.* 188: 6287–6299.

63. Roussel, L., F. Houle, C. Chan, Y. Yao, J. Bérubé, R. Olivenstein, J. G. Martin, J. Huot, Q. Hamid, L. Ferri, and S. Rousseau. 2010. IL-17 Promotes p38 MAPK-Dependent Endothelial Activation Enhancing Neutrophil Recruitment to Sites of Inflammation. *J. Immunol.* 184: 4531–4537.

64. Halwani, R., S. Al-Muhsen, and Q. Hamid. 2013. T Helper 17 Cells in Airway Diseases. *Chest* 143: 494–501.

65. Pittman, K., and P. Kubes. 2013. Damage-Associated Molecular Patterns Control Neutrophil Recruitment. *J. Innate Immun.* 5: 315–323.

66. Tang, D., R. Kang, C. B. Coyne, H. J. Zeh, and M. T. Lotze. 2012. PAMPs and DAMPs: signal 0s that spur autophagy and immunity. *Immunol. Rev.* 249: 158–175.

67. Moretti, J., S. Roy, D. Bozec, J. Martinez, J. R. Chapman, B. Ueberheide, D. W. Lamming, Z. J. Chen, T. Horng, G. Yeretssian, D. R. Green, and J. M. Blander. 2017. STING Senses Microbial Viability to Orchestrate Stress-Mediated Autophagy of the Endoplasmic Reticulum. *Cell* 171: 809-823.e13.

68. Chipurupalli, S., U. Samavedam, and N. Robinson. 2021. Crosstalk Between ER Stress, Autophagy and Inflammation. *Front. Med.* 8: 758311.

69. Niven, J., N. Madelon, N. Page, A. Caruso, G. Harlé, S. Lemeille, C. A. Seemayer, S. Hugues, and M. Gannagé. 2019. Macroautophagy in Dendritic Cells Controls the Homeostasis and Stability of Regulatory T Cells. *Cell Rep.* 28: 21-29.e6.

70. Peral de Castro, C., S. A. Jones, C. Ní Cheallaigh, C. A. Hearnden, L. Williams, J. Winter, E. C. Lavelle, K. H. G. Mills, and J. Harris. 2012. Autophagy Regulates IL-23 Secretion and Innate T Cell Responses through Effects on IL-1 Secretion. *J. Immunol.* 189: 4144–4153.

71. Cho, M.-L., J.-W. Kang, Y.-M. Moon, H.-J. Nam, J.-Y. Jhun, S.-B. Heo, H.-T. Jin, S.-Y. Min, J.-H. Ju, K.-S. Park, Y.-G. Cho, C.-H. Yoon, S.-H. Park, Y.-C. Sung, and H.-Y. Kim. 2006. STAT3 and NF-κB Signal Pathway Is Required for IL-23-Mediated IL-17 Production in Spontaneous Arthritis Animal Model IL-1 Receptor Antagonist-Deficient Mice. *J. Immunol.* 176: 5652–5661.

763 72. Sutton, C., C. Brereton, B. Keogh, K. H. G. Mills, and E. C. Lavelle. 2006. A crucial role for interleukin (IL)-1 in the
764 induction of IL-17–producing T cells that mediate autoimmune encephalomyelitis. *J. Exp. Med.* 203: 1685–1691.

765

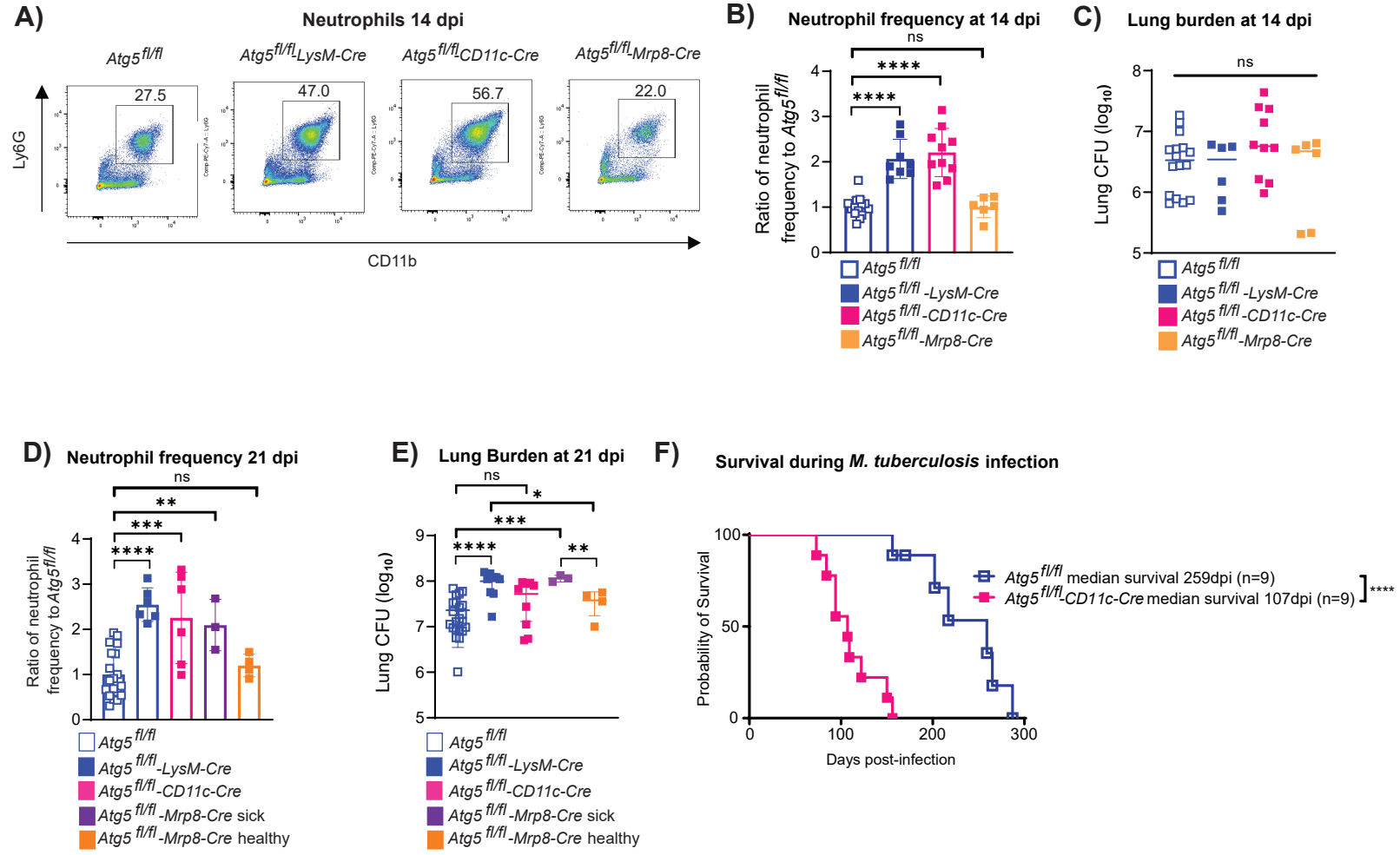

Figure 2.

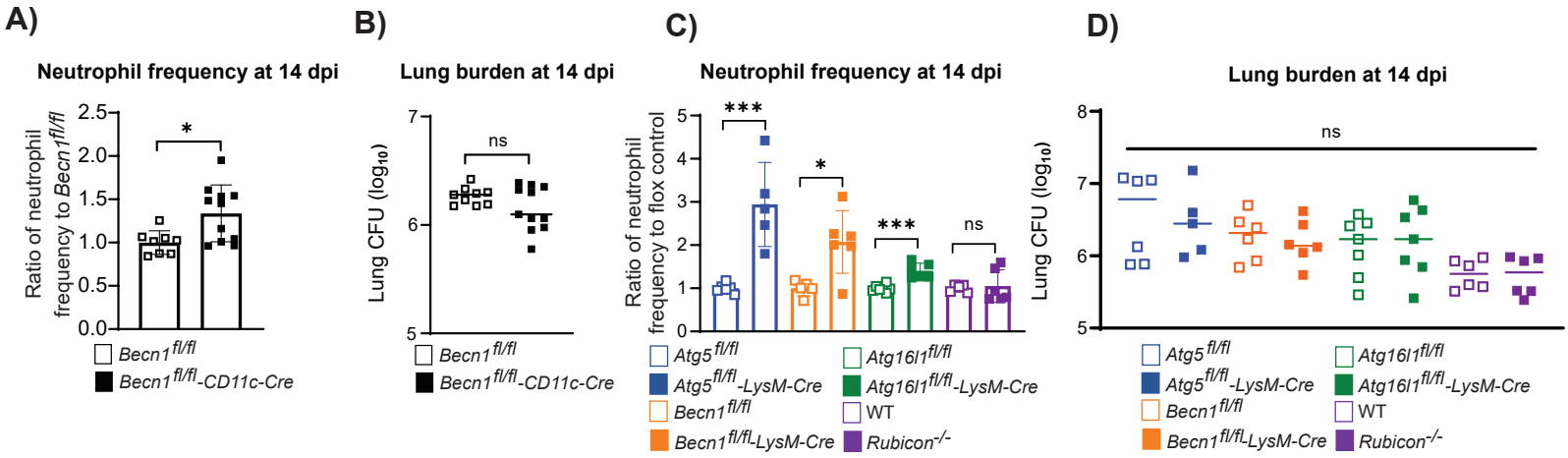

Figure 3.

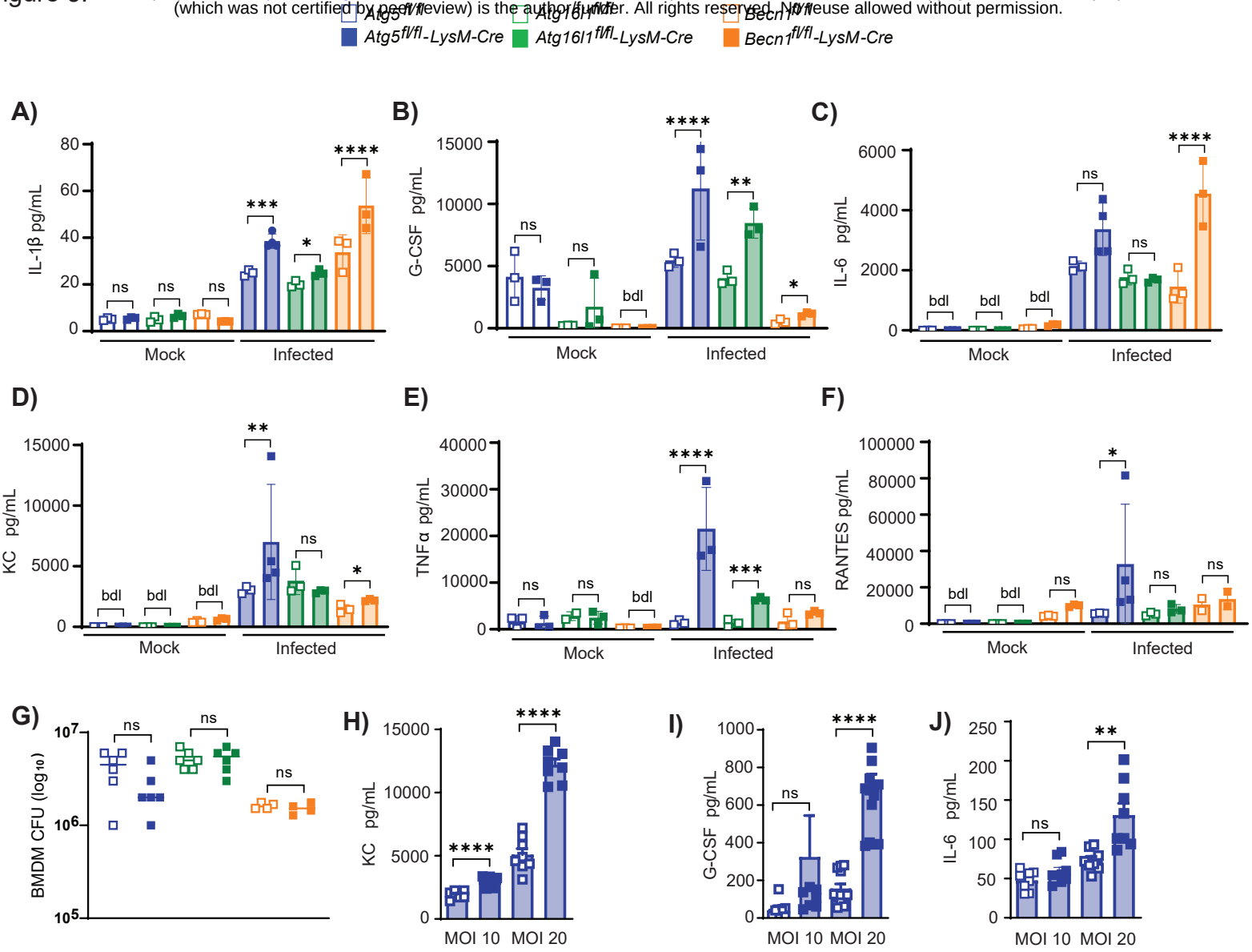

Figure 4.

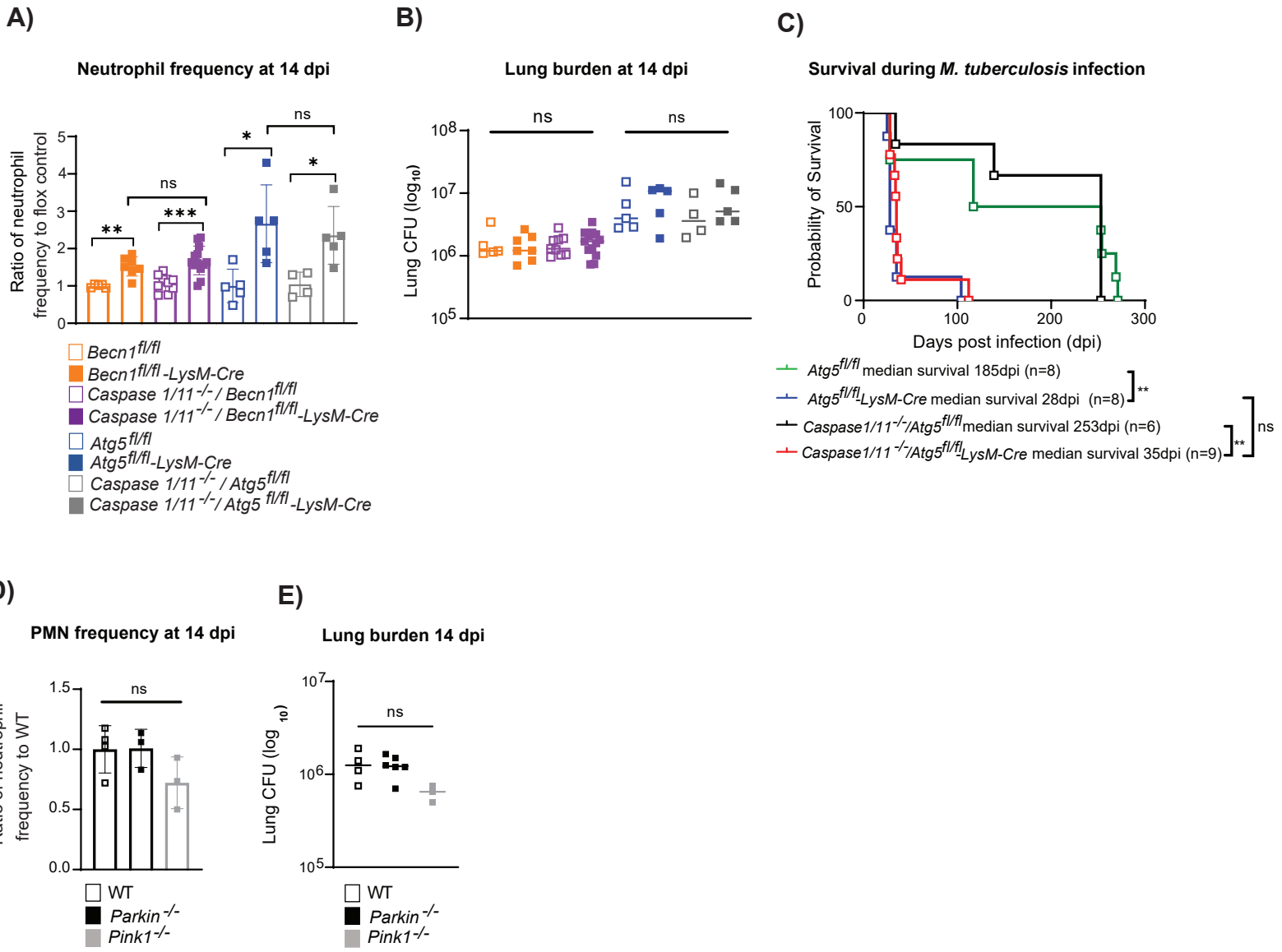

Figure 5.